ACS OMEGA

Article

Cite This: ACS Omega 2019, 4, 3012−3019

http://pubs.acs.org/journal/acsodf

Polysulfonate Cappings on Upconversion Nanoparticles Prevent Their Disintegration in Water and Provide Superior Stability in a Highly Acidic Medium

Nestor Estebanez,[†] María González-Béjar,*[,†,‡] and Julia Pérez-Prieto*[,†,‡]

[†]Instituto de Ciencia Molecular (ICMol) [‡]Departamento de Química Orgánica, Universitat de València, C/Catedrático José Beltrán, 2, 46980 Paterna, Valencia, Spain

Supporting Information

ABSTRACT: The stability of organic cappings on hexagonal $NaYF_4$:Ln^{3+} upconversion nanoparticles (UCNPs) is crucial for their luminescence efficiency in aqueous solutions. The capping removal quickens as the acidity of the medium increases. We demonstrate here that polysulfonates, namely poly(2-acrylamido-2-methyl-1-propanesulfonate) (PAMPS) and poly(sodium 4-styrene sulfonate) (PSS), remain anchored to the surface of $NaYF_4$:Yb^{3+},Er^{3+}/Tm^3 UCNPs even at a pH as low as 2 due to strong acidity of the sulfonate anchoring groups (pK_a of ca. −3). Bare UCNPs progressively disintegrate into their compositional F^-, Na^+, Y^{3+}, and Ln^{3+} ions. Their disintegration is particularly worrying in highly diluted dispersions of nanoparticles because both the lanthanide ions and/or the bare UCNPs can cause undesirable interference in a chemical or biological environment. Remarkably, the UC@PSS nanohybrid is particularly chemically stable, exhibiting an amazingly low release of Y^{3+} and Ln^{3+} ions for up to 96 h in highly diluted water dispersions (10 μg/mL). Additional advantages of the use of PSS as capping layer are its biocompatibility and its high dispersibility in water, together with easy further functionalization of the UCNP@PSS nanohybrids.

INTRODUCTION

Lanthanide-doped upconversion nanoparticles (UCNPs) consist of an inert crystalline matrix doped with at least two types of trivalent lanthanide ions (Ln), such as Yb^{3+} and Er^{3+}, one of which absorbs near-infrared (NIR) light and transfers it to the other, which emits photons of higher energy than those absorbed.[1,2] Fluorine-containing matrices are the most common as they have low phonon energies, and those with a hexagonal phase (β) are more thermodynamically stable than those with a cubic phase (α). For example, β-$NaYF_4$:Yb^{3+},Er^{3+}/Tm^{3+} UCNPs are colorless and, after NIR-excitation with a low-power continuous-wave diode laser, can produce large anti-Stokes shifted (red and green) narrow-band fluorescence emissions and even NIR-to-NIR upconversion, which makes deep-tissue imaging possible. These features, together with the fact that they do not undergo photobleaching or photoblinking and in view of their very low toxicity, make UCNPs of high relevance in biological and technological applications.

However, disintegration of α- and β-$NaYF_4$:Ln UCNPs in water has recently been reported,[3] especially in highly diluted nanoparticle suspensions.[4,5] As they progressively disintegrate, their upconversion luminescence intensity usually decreases due to the loss of active Ln ions from the host matrix, and their toxicity increases due to the release of F^-, Ln^{3+}, and Y^{3+} ions. The disintegration of $NaYF_4$:Ln UCNPs leads to the release of compositional ions, some of which are (cyto)toxic (particularly, fluoride ions).[6] In addition, toxicology studies on rats have shown that lanthanide chlorides such as that of ytterbium tend to accumulate in the liver, bones, and spleen; in the liver, they can interact with proteins, affecting enzyme activity and physiological function.[7]

The disintegration of these UCNPs is concentration- and pH-dependent. In concentrated suspensions, equilibrium is achieved with minimal disintegration, and the change in the luminescence intensity is also negligible, whereas in diluted (μM) samples, the nanoparticles can disintegrate almost completely, thereby reaching the solubility equilibrium. In terms of the acidity of the medium, pristine UCNPs (i.e., oleate-capped UCNPs) are unstable in acidic physiological fluids such as lysosomes (pH ca. 4.5−5.0).[8] It has to be taken into account that at pH = 4, carboxylate-capped UCNPs lose their protected capping; in fact, bare UCNPs can be prepared by treatment of the NPs with HCl at pH 4, which protonates the oleate ligand resulting in the release of oleic acid.[9] This capping removal does not only apply to carboxylate ligands but also to many other types of ligands.

Soukka et al.[4] have recently put forward a solution to prevent the disintegration of UCNPs in highly diluted water dispersions (few micrograms per milliliter); their solution is made by adding fluoride ions, which have a high impact on the solubility equilibrium, eventually decelerating the disintegration of poly(acrylic acid)-capped UCNPs. Unfortunately, this strategy needs a considerably high concentration (mM) of fluoride, which, from the point of view of their use in live cells, is not advisable due to its (cyto)toxicity.[10]

The requirement of ligands to remain on the nanoparticle surface in a broad range of pH values, and particularly, at low pH values (such as that of stomach acid, which is close to 2), is that they possess strongly ionizable anchoring groups. These

Received: October 30, 2018
Accepted: January 21, 2019
Published: February 11, 2019

DOI: 10.1021/acsomega.8b03015
ACS Omega 2019, 4, 3012−3019

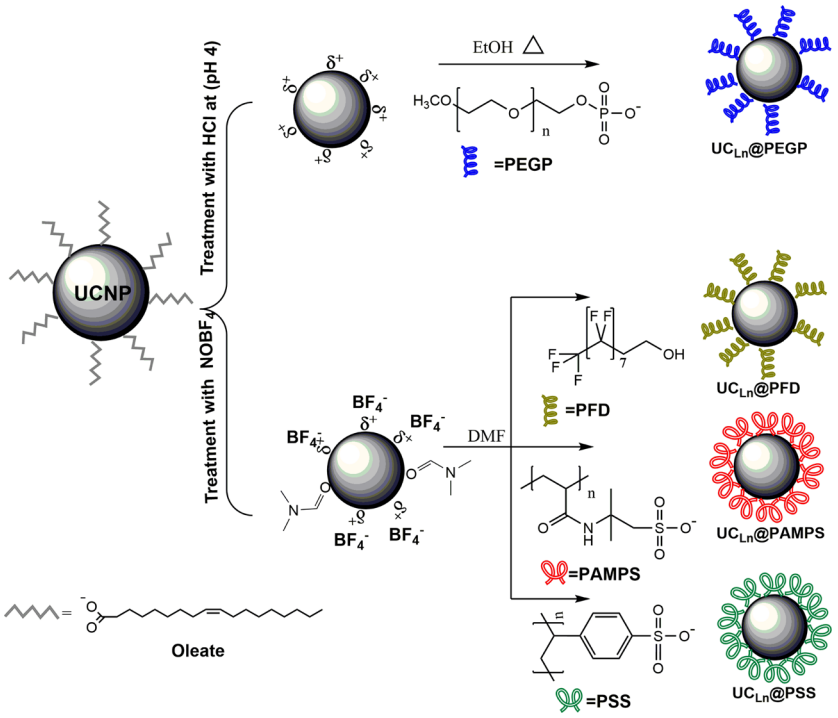

Figure 1. Scheme of the synthetic procedure used for building the coated upconversion nanoparticles (UC_{Ln}@PAMPS, UC_{Ln}@PSS, UC_{Ln}@PEGP, and UC_{Ln}@PFD) and structure of the ligands: poly(2-acrylamido-2-methyl-1-propanesulfonate) (PAMPS); polystyrene sulfonate (PSS); mPEG5K-phosphate (PEGP); and 1*H*,1*H*,2*H*,2*H*-perfluoro-1-decanol (PFD).

groups may help modulate the extent to which the nanoparticle is absorbed in the organism (e.g., the gastrointestinal tract) and its bioavailability (e.g., nanoparticle ionization decreases absorption).[13] An organic shell completely covering and strongly anchored to the UCNP surface might prevent undesirable interference in biological environments (interactions with different blood components or any biological fluids, formation of a protein corona).[11,12]

Xia et al. demonstrated that a multichelating phosphonate coating (ethylenediamine tetra(methylene phosphonate), EDTMP) can prevent the disintegration in water of $NaYF_4$:Er^{3+},Yb^{3+} NPs (200 μg NP/mL), whereas UCNPs capped with monophosphonates and citrate are drastically damaged. These facts can be attributed to the strong coordination of EDTMP to the UCNP surface as a consequence of the affinity of the phosphonate group to the cations at the surface, combined with the hexadentate binding of the ligand by means of its four phosphonates and two amine groups. The EDTMP-capped NPs showed a high resistance to disintegration when incubated in phagolysosomal simulated fluid (pH 4.5) for 24 h. It is worth mentioning that these studies were performed with relatively high concentrations of NPs.[14]

Many applications of UCNPs require that the NPs possess an organic capping that (i) provides them with high dispersibility in water, (ii) protects them from disintegrating in water at neutral pH and/or acid media, (iii) makes their further functionalization possible and/or impedes the UCNPs from causing any undesirable interference in the (chemical or cellular) environment, and (iv) is biocompatible.

With the aim of obtaining more stable UCNPs in water, we focused on coating the UCNP surface with multichelating, strongly acidic ligands, specifically, polysulfonates. The sulfonic group is a strong acid (pK_a of ca. −3) which is virtually ionized throughout the entire range of pH values; the sulfonate group has three potential coordination sites and can be effectively grafted to the UCNP surface.[15]

We demonstrate here that polysulfonates, such as polystyrene sulfonate (PSS), remain anchored to the surface of $NaYF_4$:Ln^{3+} UCNPs even at pH of ca. 2 and that highly diluted water dispersions of the UCNP@PSS nanohybrid (10 μg/mL) show an amazingly low release of Y^{3+} and Ln^{3+} ions for up to 96 h.

RESULTS AND DISCUSSION

Synthesis and Characterization of the Polymer-Capped UCNPs. First, different organic ligands with functional groups able to coordinate Ln^{3+} ions, specifically, phosphate, sulfonate, and even fluoride,[i] [16−22] were used for coating the UCNP surface with the purpose of comparing the resistance to acids of the corresponding capping under a strong acid medium (pH of ca. 2). Two types of upconversion nanoparticles (UCNPs), namely $NaYF_4$:Yb^{3+},Er^{3+} and $NaYF_4$:Yb^{3+},Tm^{3+}, were synthesized by thermal decomposition with oleic acid and 1-octadecene at high temperature following a slightly modified well-known protocol. A batch of oleate-capped β-$NaYF_4$:Yb^{3+},Er^{3+} (UC_{Er}@OA) and two different batches of β-$NaYF_4$:Yb^{3+},Tm^{3+} (UC_{Tm1}@OA and UC_{Tm2}@OA) were used for the studies reported here.[23] Experimental details, X-ray diffraction (XRD) data, transmission electron microscopy (TEM) images, size distribution histograms, and inductively coupled plasma mass spectrometry (ICP-MS) analyses can be found in the Supporting Information (Figures S1 and S2 and Table S1). TEM images showed that UC_{Tm1}@OA, UC_{Tm2}@OA, and UC_{Er}@OA NPs were uniform hexagonal prisms, and their average sizes were (22.7 ± 0.9) × (20.3 ± 1.0) nm, (32.9 ± 1.9) × (22.4 ± 2.2) nm, and (46.7 ± 1.8) × (28.6 ± 1.4) nm, respectively.

DOI: 10.1021/acsomega.8b03015
ACS Omega 2019, 4, 3012−3019

Next, bare UCNPs were prepared by treatment of the oleate-capped NPs either with HCl at pH 4 or by addition of $NOBF_4$ to lead to $UC_{Ln}@BF_4$.[24,25] The low binding affinity of the BF_4^- anion to the UCNP surface together with the strong coordination capability of the Ln^{3+} ions makes the secondary surface modification possible. Then, the as-prepared bare UCNPs were reacted with the selected ligands, namely (i) poly(2-acrylamido-2-methyl-1-propanesulfonate) (PAMPS), (ii) poly(sodium 4-styrene sulfonate) (PSS) with an M_w of 70000, (iii) mPEG5K-phosphate (PEGP), and (iv) 1*H*,1*H*,2*H*,2*H*-perfluoro-1-decanol (PFD) (Figure 1), to afford UC_{Ln}@PAMPS, UC_{Ln}@PSS, UC_{Ln}@PEGP, and UC_{Ln}@PFD NPs, respectively (see the Materials and Methods section for further details).

The successful coating of the UC_{Ln} surface with PAMPS, PSS, PEGP, and PFD was corroborated by HRTEM, FTIR (Figures 2 and 3), and TGA (Figure S3−S5 in the Supporting Information). Thus, Figure 2 shows high-resolution TEM (HRTEM) images of representative samples of the four coated UC_{Tm} NPs where the presence of an organic layer can be observed around the surface of the inorganic NPs (see Figure S6 for coated UC_{Er} NPs). The thickness of the capping was 2.5 ± 0.1 nm in the case of UC_{Tm}@PAMPS, 1.6 ± 0.3 nm for UC_{Tm}@PSS, and 2.2 ± 0.3 nm for UC_{Tm}@PEGP. The thinner capping (ca. 0.7 nm ± 0.3 nm) of the UC_{Tm}@PFD NPs is consistent with the smaller size of the perfluoroalkanol ligand. As expected, the nanoparticle sizes after surface functionalization remained identical to that of the parent UC_{Ln} NP.

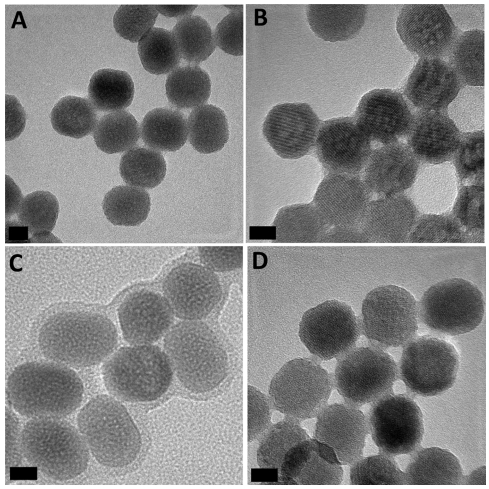

Figure 2. Representative HRTEM images of (A) UC_{Tm1}@PAMPS, (B) UC_{Tm1}@PSS, (C) UC_{Tm2}@PEGP, and (D)UC_{Tm1}@PFD. Scale bar 10 nm.

The FTIR spectrum of the samples (see Figure 3, left) clearly showed the characteristic signals of each ligand coating the UC_{Ln} surface; briefly,(i) the C−H stretching vibration around 2880 cm^{-1} in all of them, (ii) the C−O stretching vibration at 1110 cm^{-1} associated with the backbone of the PEG chains and the vibration at ca. 1240 cm^{-1} typical of P═O in PEGP, (iii) the two bands centered at ca. 1220 and 1045 cm^{-1}, which correspond to the stretching vibration (asymmetric and symmetric, respectively) of the S═O groups in the sulfonated polymers, and the bands at ca. 1700 cm^{-1} attributed to C═O of the amide in PAMPS, and (iv) the multiple strong bands in the range of 1350−1100 cm^{-1} assigned to C−F stretching modes of the perfluoroalkyl chain of PFD.[26] In addition, the comparison between the spectra of the ligand-coated UCNPs and that of the corresponding ligand (not shown) evidenced the effect of the anchoring to the NP surface on the ligand vibrations, for example, fewer bands in the 1550 to 1000 cm^{-1} region due to the interaction of fluorine atoms with the UCNP surface, specifically with Y^{3+} and/or Ln^{3+} ions.

In fact, lanthanide shift reagents have been applied to the study of alkyl fluorides by ^{1}H-NMR spectroscopy. Important findings are that the chemical shift induced by Yb^{3+} shift reagents decreases as the distance from the fluorine atom to the observed nucleus increases, and the resolution of the shifted resonances is poor for the nucleus closest to the fluorine center.[20] These shifts have been attributed to the formation of fluorine-coordinated lanthanide complexes. ^{19}F-NMR spectra of the ligand and UC_{Ln}@PFD were recorded in deuterated-methanol (see Figure S7) because the ^{19}F-NMR spectra can be useful to determine the type of anchoring of PFD to the NP surface (via multidentate chelation or an active functional group located at the end of the chain, termed brush-like interaction). Both spectra showed seven bands at −82.85, −115.15, −123.15, −123.40, −124.20, −125.25, and −127.75 ppm; the most significant difference between them was that the multiplet at −82.85 ppm in PFD, assigned to CF_3, turned into a broad band in UC_{Ln}@PFD. This is consistent with the interaction of PFD with the NP surface via the CF_3 group, although from the negligible changes in the chemical shifts of the ligand, it can be inferred that this interaction is weak.

Thermogravimetric analyses (TGA) of the UC_{Ln}@ligand NPs, namely UC_{Ln}@PAMPS, UC_{Ln}@PSS, UC_{Ln}@PEGP, and UC_{Ln}@PFD NPs, were carried out to determine the presence and amount of ligand bound to the nanoparticle surface (see Figure S5 in the Supporting Information). A weight loss of ca. 10 wt % was observed at temperatures below 750 °C for the four of them, and it can be attributed to the organic capping.

The emission spectra (λ_{ex} = 975 nm) of UC_{Tm1}@PAMPS, UC_{Tm1}@PSS, UC_{Tm2}@PEGP, and UC_{Tm1}@PFD NPs, as well as those of UC_{Er}@PAMPS and UC_{Er}@PSS, are shown in Figure S8 (see the Supporting Information). The UC_{Tm} NPs showed the typical Tm^{3+} emission bands: four of them below 500 nm [$^1I_6 \rightarrow {}^3F_4$ (at 345 nm),$^1D_2 \rightarrow {}^3H_6$ (at 368 nm),$^1D_2 \rightarrow {}^3F_4$ (at 450 nm), and $^1G_4 \rightarrow {}^3H_6$ (at 475 nm) transitions] and other three bands at 650, 700, and 800 nm. In the case of the UC_{Er} NPs, the three more intense emission bands can be observed in the green spectral region centered at λ_{em} at 525 ($^2H_{11/2}/^4I_{15/2}$ transition) and 545 nm ($^4S_{3/2}/^4I_{15/2}$ transition) and in the red spectral region centered at λ_{em} at 660 nm ($^4F_{9/2}/^4I_{15/2}$ transition).

As stated before, our purpose was to evaluate the efficiency of different ligands to protect the UC_{Ln} surface even in a highly acidic aqueous medium as low as pH 2. It is equally important to prevent the disintegration of UC_{Ln} in highly diluted water dispersions (few micrograms per milliliter). Both occurrences, the loss of the organic capping and the disintegration of the inorganic core, can cause undesirable interference in a chemical or biological environment. The next two sections are devoted to presenting and discussing the results after acid treatment of the four coated UC_{Ln} NPs as well as the extraordinary chemical and photophysical stability of the sulfonate-coated NPs in water.

Stability of the Polymer Capping of UC_{Ln} in Strongly Acidic Media. Each coated UC_{Ln} was dispersed in milliQ-water, and the pH of the colloidal dispersion was measured at room temperature. Then, the sample was acidified (see the

DOI: 10.1021/acsomega.8b03015
ACS Omega 2019, 4, 3012−3019

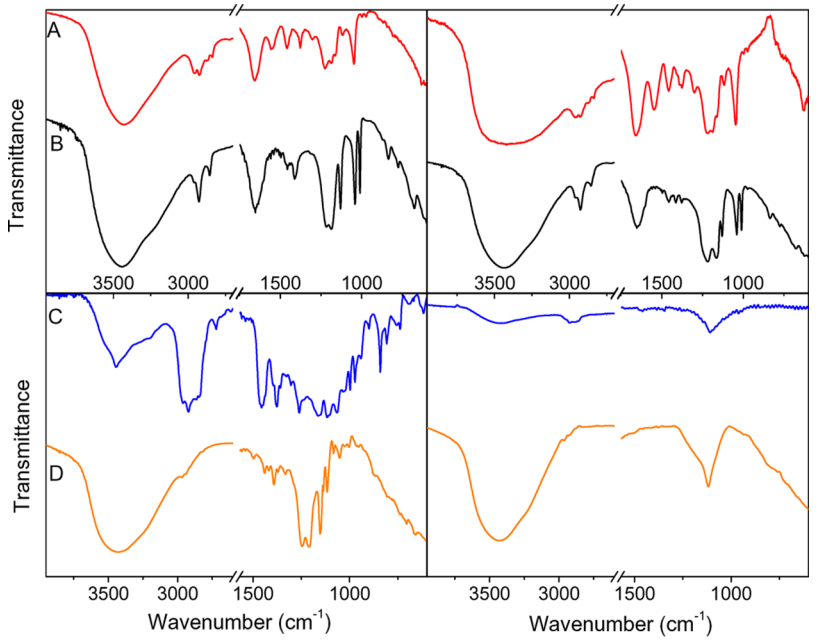

Figure 3. FTIR spectra of (A) UC_{Tm1}@PAMPS, (B) UC_{Tm1}@PSS, (C) UC_{Tm2}@PEGP, and (D)UC_{Tm1}@PFD before (left) and after (right) acid treatment.

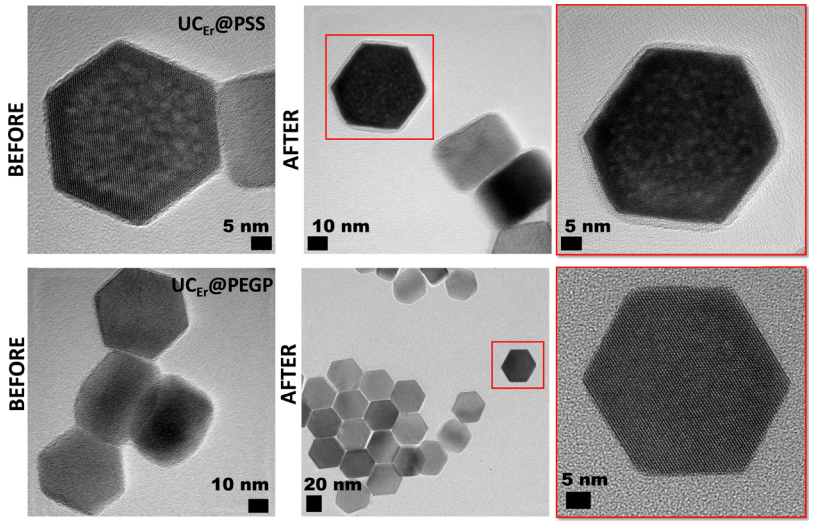

Figure 4. Representative HRTEM images of UC_{Er}@PSS (top) and UC_{Er}@PEGP (bottom), before (left) and after (center) acid treatment; expanded image of the nanoparticles is shown in the red square in the center images (right).

Materials and Methods section) with HCl solution down to pH 2, and its emission was measured after 12 h (see Supporting Information, Figures S9 and S10). Next, the sample was centrifuged and washed with milliQ-water, eventually obtaining a solid, which was analyzed by FTIR. Figure 3 (right) shows the FTIR spectra after acid treatment and reveals that only those cappings with sulfonate groups remain anchored to the surface of the UC_{Ln} NPs, that is, UC_{Tm}@PAMPS and UC_{Tm}@PSS, while no capping was then distinguished for UC_{Tm}@PEGP and UC_{Tm}@PFD (see Figure S11 for the UC_{Er} nanohybrids). Figure 4 shows HRTEM images of UC_{Er}@PSS and UC_{Er}@PEGP captured after acid treatment compared to those before such treatment (see Figure S12 for other samples). The fact that the sulfonated ligands remained anchored to the UCNP surface in strong acid medium is relevant from the point of view of UCNP applications, because the maintenance of the organic capping is crucial for its performance. Remarkably, polysulfonate-capped UC_{Ln} were emissive at acidic pH values (Figure S13). The failure of UC_{Ln}@PEGP and UC_{Ln}@PFD to maintain the capping under strong acid media can be attributed to acid-induced weakening of the coordination of the ligand to the NP surface (see Footnote *ii* for UC_{Ln}@PFD).[27,28]

The change in the NP surface charge as a consequence of the acid treatment was consistent with the variation of the zeta potential of the NPs (see Table S2 in the Supporting Information). Before and after acid treatment, UC_{Ln} and UC_{Ln}@BF_4 show positive values (≈19 mV), whereas those of UC_{Ln}@PSS and UC_{Ln}@PAMPS are negative (≈−31 and −26 mV, respectively, due to the anionic polymers). However, UC_{Ln}@PEGP and UC_{Ln}@PFD show either slightly negative (≈−3 mV) or slightly positive (≈11 mV) zeta potential values,

DOI: 10.1021/acsomega.8b03015
ACS Omega 2019, 4, 3012−3019

Table 1. Total Molar Amount of Dissolved Lanthanide Ions[a] from UC_{Er}@PSS, UC_{Er}@PAMPS, and Naked UC_{Er}[b]

		supernatant (μM)[c]				
sample	time (h)	Ln^{3+}total	Ln^{3+} loss (%)[d]	Er^{3+}	Y^{3+}	Yb^{3+}
UC_{Er}	24	4.63	4.41	0.0930	3.77	0.780
	48	6.44	6.05	0.120	5.29	1.03
	72	2.70	2.56	0.0536	2.19	0.458
	96	0.200	0.21	4.65×10^{-3}	0.123	0.0712
UC_{Er}@PSS	24	**0.0422**	0.0555	1.13×10^{-3}	0.0327	8.32×10^{-3}
	48	**0.376**	0.479	6.16×10^{-3}	0.307	0.0625
	72	**0.280**	0.346	4.64×10^{-3}	0.239	0.0363
	96	**0.352**	0.420	3.82×10^{-3}	0.317	0.0319
UC_{Er}@PAMPS	24	1.39	4.03	0.0275	1.12	0.244
	48	1.69	4.97	0.0340	1.32	0.331
	72	1.56	4.51	0.0307	1.26	0.269
	96	0.214	0.669	4.61×10^{-3}	0.151	0.0588

[a]Ln^{3+}: Y^{3+}, Yb^{3+}, and Er^{3+} ions. [b]10 μg/mL, incubated in milliQ-water up to 96 h. [c]Determined by ICP-MS. [d]Percentage of dissolved Ln^{3+} from the starting UC_{Er} nanoparticle.

respectively, before acid treatment (dispersed in milliQ-water), but their zeta potential was similar to that of the bare UC_{Ln} after acid treatment (see Table S3), which evidences the removal of their capping ligand. Indeed, DLS showed no sign of aggregation for these nanohybrids (e.g., UC_{Er}@PSS in Figure S14).

Chemical and Photophysical Stability of the Sulfonate-Coated UC_{Er} NPs in Water. The disintegration of the inorganic core of UC_{Er} in highly diluted aqueous dispersions (10 μg/mL, 8mL) was evaluated for those systems that showed stable organic capping upon acid treatment, that is, UC_{Er}@PSS and UC_{Er}@PAMPS. For this purpose, the dissolution of UC_{Er}@PSS and UC_{Er}@PAMPS into their constituents, Y^{3+}, Yb^{3+}, and Er^{3+}/Tm^{3+}, was measured by inductively coupled plasma mass spectrometry (ICP-MS), which is an appropriate quantification method for the release of the ions from the inorganic nanoparticles,[4] and the process was monitored for up to 96 h. For comparative purposes, the disintegration of the bare UC_{Er} NPs was also analyzed. Briefly, 8 mL of each colloid (10 μg/mL) was vortexed (200 rpm/min) at room temperature for 24h. Then, a 2mL aliquot was taken, and after centrifugation (15000 rpm/min, 20 min) and filtration, the supernatant was analyzed by ICP-MS. This process was repeated at 24 h intervals up to 96 h with aliquots taken from the remaining solution to determine the chemical stability of the nanoparticles (see results in Table 1 and a schematic representation of the process in Figure S15 in the Supporting Information).

Data in Table 1 show that the two sulfonated polymers clearly prevented the disintegration of the NP when compared to that of the bare NP (there was a 100-fold less dissolved Ln^{3+} total concentration for the PSS-capped nanoparticle compared to the bare UC_{Er} after 24 h), but PSS was more effective than PAMPS. This could be attributed to the high hydrophobicity of the polystyrene moiety in PSS and/or the higher content of sulfonate groups in this polymer that have a stronger binding capacity than the amide in PAMPS.

An interesting observation was the decrease in the Ln^{3+} concentration in the supernatant arising from the disintegration of the bare UC_{Er} NPs under prolonged incubation in water, specifically 72 and 96 h (Table 1). This may be due to the deposition of the ions as complexes on the NP surface. In fact, ICP-MS results of the solid residue in the centrifuged samples at 24, 48, 72, and 96 h showed how the ratio between lanthanides in the bare UC_{Er} nanoparticles was changing over time (Figure S16). Interestingly, the ratio of Y increased, but the ratio of both Yb and Er decreased. This explains why the total ion concentration in the supernatant decreased with extended suspension times. This process was much less evident in UC_{Er}@PAMPS, once again corroborating the high chemical stability provided by PAMPS to the inorganic nanoparticle. In addition, the structural integrity of the bare UCEr and UCEr@PPS nanoparticles was monitored by TEM for up to 96 h. These experiments show the drastic corrosion of the bare nanoparticles. These images also demonstrate the beneficial effect of the polysulfonate in preventing the nanoparticle disintegration (Figure S17).

Finally, the photophysical stability, that is, the upconversion luminescence in aqueous media of UC_{Er}@PSS, UC_{Tm}@PSS, and naked UC_{Er} (particle concentration of 5 μg/mL), was evaluated. The luminescence spectra (λ_{ex} = 975 nm) were registered after incubating the nanoparticles for 24 h (every 90 min for the first 8 h and then at 24 h) in pure water while being slowly shaken. The area under the curve was calculated for each measurement. Figure 5 clearly shows a loss of emission intensity for bare UC_{Er}. As explained above, this fact could be attributed not only to the loss of doping ions (Yb/Er) and disintegration of UC_{Er} but also to adsorption of some of the "dissolved" ions on the nanoparticle surface. Undoubtedly, the best photostability was observed for UC_{Ln}@PSS, which

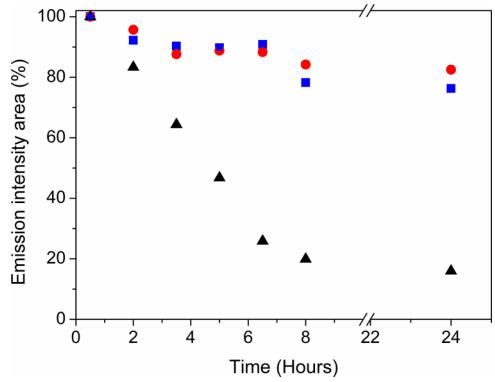

Figure 5. Emission intensity (area under the curve) over time for water dispersions of 5 μg/mL UC_{Er}@PSS (blue squares), UC_{Tm1}@PSS (red circles), and naked UC_{Er} (black triangles).

DOI: 10.1021/acsomega.8b03015
ACS Omega 2019, 4, 3012−3019

wholly agrees with the lower dissolution of lanthanide ions in water as observed by ICP-MS. Therefore, coating the UC_{Er} with PSS not only allowed chemical stability in highly acidic medium but also prevented dissolution of its inorganic UC_{Er} core into its lanthanide ions and preserved the upconversion emission for longer periods.

CONCLUSIONS

In summary, we demonstrate here that not only do highly acidic polysulfonates remain strongly coordinated to the $NaYF_4:Ln^{3+}$ UCNPs in strong acidic media and provide the nanoparticle with high dispersibility in water as well as additional functionality but also these cappings meet the requirements for an adequate protection of $NaYF_4:Ln^{3+}$ UCNPs to preserve their integrity in highly diluted water dispersions. These are especially interesting results because an adequate capping can preserve the luminescence properties of the UCNPS as well as avoid the (bio)toxicity caused by the disintegration of the nanoparticles into toxic ions, such as fluoride ions. The next step is to study the capacity of the sulfonate capping to preserve the chemical stability and photophysical features of the nanoparticles in highly diluted, strongly acidic solutions; these studies are ongoing and will be reported in due course.

MATERIALS AND METHODS

The chemicals used for the nanoparticle syntheses were lanthanide chlorides ($YCl_3·6H_2O$, $YbCl_3·6H_2O$, $ErCl_3·6H_2O$, $TmCl_3·6H_2O$, and $NdCl_3·6H_2O$ (>99.9%, all of them)), 1-octadecene (95%), oleic acid (70%), and NaOH and NH_4F (99.99%). All of these chemicals were purchased from Sigma-Aldrich and used as received without previous purification. The chemicals used for the coatings were poly(2-acrylamido-2-methyl-1-propanesulfonate, (M_w of ∼25,000) (see the Supporting Information), poly(sodium 4-styrene sulfonate), PSS (M_w of ∼70,000, Sigma-Aldrich), mPEG5K-phosphate (Sigma-Aldrich), and 1*H*,1*H*,2*H*,2*H*-perfluoro-1-decanol (>97%, Alfa Aesar). Transmission electron microscopy (TEM) images were obtained using a Jeol 1010 microscope operating at 100 kV equipped with a digital camera (AMT RX80; 8 megapixels). For the preparation of the samples, 10 μL of a 0.5 mg·mL^{-1} solution of the UCNPs was left to dry under vacuum at room temperature on a Formvar/carbon film supported on a 300-mesh copper grid. High-resolution transmission electron microscopy (HRTEM) images were recorded using a TECNAI G2 F20 microscope operating at 200 kV (point resolution of 0.24 nm) and equipped with a CCD GATAN camera. XRD analyses were performed on a Bruker D8 Advance A25 diffractometer using Cu Kα (λ = 1.54060 Å) radiation at a voltage of 40 kV and 30 mA, and a LynxEye detector. The powder diffraction pattern was scanned over the angular range of 2−80° (2θ) with a step size of 0.020° at room temperature. All FTIR spectra were obtained using an FTIR Thermo Nicolet Nexus spectrophotometer at room temperature with 64 scans and a resolution of 4 cm^{-1} between 400 and 4000 cm^{-1}. The TGA analyses were carried out using a TGA 550 from TA instruments with an operative temperature range 50-800 °C and 0.1 microgram sensitivity. The samples were heated from 50 to 750°C, with an increase of 5°C·min^{-1} and under air flux of 50 mL·min^{-1}. The pH measurements were carried out by using a pH meter (GLP21). Centrifugation was carried out in a Thermo-Scientific Legend XIR. ICP-MS analyses were carried out using an ICP-MS Agilent 7900. Dynamic light scattering and zeta potential (ζ) analyses were performed on a Zetasizer Nano ZS from Malvern.

Synthesis of UC_{Ln} Coated with Polystyrene Sulfonate (UC_{Ln}@PSS). A mixture of 2 mL of $UC_{Ln}@BF_4$ dispersed in DMF (50mg/mL), DMF (3 mL) and PSS (1.7 mL) was kept under vigorous stirring at 60 °C. This turbid mixture was further stirred for 24 h. Then, the BF_4^- capping was replaced by PSS. The dispersion was centrifuged for 20 min at 15000 rpm, and the supernatant was discarded. Then, the coated UC_{Ln}@PSS NPs were redispersed in 10 mL of milliQ-water and centrifuged for 15 min at 15000 rpm to remove excess PSS. This step was repeated three times. Finally, the pellet was redispersed in DMF (5 mL) and centrifuged for 3 min at 2000 rpm to get rid of larger agglomerates.

Synthesis of UC_{Ln} Coated with Poly(2-acrylamido-2-methyl-1-propanesulfonate) (UC_{Ln}@PAMPS). To 2 mL of a $UC_{Ln}@BF_4$ dispersion (50mg/mL DMF), 500 mg of AMPS dissolved in 3 mL of DMF was added and kept under vigorous stirring at 60 °C for 24 h to displace BF_4^- and obtain UC_{Ln}@PAMPS. The following steps were identical to those described above for purification of UC_{Ln}@PSS.

Synthesis of UC_{Ln} Coated with mPEG5K-Phosphate (UC_{Ln}@PEGP). Naked UC_{Ln} NPs were coated with mPEG5K-phosphate by following the procedure previously described.[29,30] In short, approximately 50 mg of naked UC_{Ln} dispersed in 2 mL of absolute ethanol was placed into a glass vial, and 300 mg of PEG-phosphate ligand was added to it. The vial was capped tightly, and the resulting solution was stirred overnight at 60 °C. Then, it was cooled to room temperature, UC_{Ln}@PEGP NPs were collected via centrifugation at 15000 rpm for 20 min, and the supernatant was discarded. The pellet was redispersed in 10 mL of milliQ-water and centrifuged for 15 min at 10000 rpm. This washing step was repeated in triplicate.

Synthesis of UC_{Ln} Coated with 1*H*,1*H*,2*H*,2*H*-Perfluoro-1-decanol (UC_{Ln}@PFD). To 2 mL of a $UC_{Ln}@BF_4$ dispersion in DMF (50mg/mL), 500 mg of 1*H*,1*H*,2*H*,2*H*-perfluoro-1-decanol dissolved in 3 mL of DMF and four drops of triethylamine were added under vigorous stirring at 50 °C for 24 h. The dispersion was centrifuged for 20 min at 15000 rpm, and the supernatant was discarded. The pellet was redispersed in 10 mL of methanol and centrifuged for 15 min at 15000 rpm twice. Additionally, it was washed two times by dispersion in 10 mL of methanol. Finally, the pellet was redispersed in 5 mL of DMF.

Steady-State Photoluminescence. Steady-state photoluminescence spectra were obtained at room temperature with a 2 nm slit width and 5 nm·s^{-1} speed scan using an SLM Amingo Bowmann series 2 (AB2) fluorometer (Microbeam, S.A.). The AB2 software (v.5.5) was used to register the data. Upconversion emission spectra were recorded by excitation at 975 ± 10 nm using a CW 975 nm diode laser (Thorlabs L975P1WJ) as an excitation source coupled to the fluorometer.

Measurement of the Nanohybrid Emission versus pH. The selected coated UC_{Ln} was dispersed in milliQ-water (5 mg × 5 mL^{-1}), and the pH of the colloidal dispersion was measured at room temperature. Subsequently, different aliquots (5 or 10 μL) of HCl solution (0.1 or 0.5M) were added, and after each addition, the pH and the emission were measured up to pH 2 or slightly lower. Next, the emission was registered again after 12 h under continuous stirring. After that, the sample was centrifuged at 15000 rpm for 20 min, and the

DOI: 10.1021/acsomega.8b03015
ACS Omega 2019, 4, 3012−3019

solid was washed twice with 5 mL of milliQ-water. After removing the supernatant, the solid was dried under vacuum, and the FTIR spectrum was registered.

Chemical Stability of UC_{Er}@PSS, UC_{Er}@PAMPS and Bare UC_{Er}@PSS in Water. A dissolution test of the UC_{Ln} NPs into its constituents Y^{3+}, Yb^{3+}, and Er^{3+}/Tm^{3+} was performed for UC_{Er}@PSS, UC_{Er}@PAMPS, and bare UC_{Er}@PSS. In each case, the colloid (8 mL, 10 μg/mL) in water was shaken (200 rpm/min) at room temperature for 24 h. Then, a 2mL aliquot was taken and centrifuged at 15000 rpm for 20 min to remove the majority of the UC_{Ln}, and the supernatant was subsequently filtered[31] by using an ACRODISC GHP 0.2 μm filter to avoid the presence of UC_{Ln}. This process was repeated three times to determine the chemical stability of the nanoparticles for up to 96 h (see results in Table 1). Finally, the supernatants were taken for analysis by ICP-MS using a spectrometer (IC-MS Agilent 7900) (see schematic representation of the process in Figure S13 in the Supporting Information).

Photophysical Stability of UC_{Ln}@PSS in Water. The effect of the Ln^{3+} ion dissolution from the UCNP on their upconversion emission was studied by following a procedure similar to that previously described.[4] Briefly, UC_{Ln}@PSS (5 μg/mL) and naked-UC_{Er} (5 μg/mL) solutions in water were prepared and stirred at room temperature. The emission intensity of these solutions was monitored by recording the emission spectrum between 0 and 24 h. Then, the area under the emission peaks was measured.

■ ASSOCIATED CONTENT

Supporting Information

The Supporting Information is available free of charge on the ACS Publications website at DOI: 10.1021/acsomega.8b03015.

Experimental procedure, zeta potential data, ICP-MS analyses, XRD, ^{19}F-NMR and TGA spectra, additional TEM images, FTIR spectra, emission spectra and emission of a water dispersion of UCNPs vs time (PDF)

■ AUTHOR INFORMATION

Corresponding Authors

*E-mail: maria.gonzalez@uv.es (M.G.-B.).
*E-mail: julia.perez@uv.es (J.P.-P.).

ORCID

María González-Béjar: 0000-0001-5434-4210
Julia Pérez-Prieto: 0000-0002-5833-341X

Notes

The authors declare no competing financial interest.

■ ACKNOWLEDGMENTS

We thank MINECO (CTQ2017-82711-P) partially cofinanced with FEDER funds, Maria de Maeztu (MDM-2015-0538), RTC-2016-5114-5 (contract NEB), RyC (MGB), and Fundación Ramón Areces for financing this research.

■ ADDITIONAL NOTES

[i]The coordination chemistry of fluorocarbon C−F moieties with metal cations has been previously reviewed in 1997 and 2004 (see refs 16 and 17). In addition, the activation of C−F bonds by bonding lanthanide ions has been reported (see refs 18 and 19).

[ii]NMR measurements combined with DFT theoretical calculations have revealed the existence of intramolecular hydrogen bonds in organofluorine-substituted derivatives of different classes of molecules (ref 27). In addition, it has been suggested that proton−fluoride interactions can play a significant role in the stabilization of conformational molecular states ,especially via cooperativity(ref 28)

■ REFERENCES

(1) Gnach, A.; Bednarkiewicz, A. Lanthanide-Doped up-Converting Nanoparticles: Merits and Challenges. *Nano Today* **2012**, *7*, 532−563.
(2) Wu, X.; Chen, G.; Shen, J.; Li, Z.; Zhang, Y.; Han, G. Upconversion Nanoparticles: A Versatile Solution to Multiscale Biological Imaging. *Bioconjugate Chem.* **2015**, *26*, 166−175.
(3) Lisjak, D.; Plohl, O.; Ponikvar-Svet, M.; Majaron, B. Dissolution of Upconverting Fluoride Nanoparticles in Aqueous Suspensions. *RSC Adv.* **2015**, *5*, 27393−27397.
(4) Lahtinen, S.; Lyytikäinen, A.; Päkkilä, H.; Hömppi, E.; Perälä, N.; Lastusaari, M.; Soukka, T. Disintegration of Hexagonal NaYF4:Yb^{3+},Er^{3+} Upconverting Nanoparticles in Aqueous Media: The Role of Fluoride in Solubility Equilibrium. *J. Phys. Chem. C* **2017**, *121*, 656−665.
(5) Dukhno, O.; Przybilla, F.; Muhr, V.; Buchner, M.; Hirsch, T.; Mély, Y. Time-Dependent Luminescence Loss for Individual Upconversion Nanoparticles upon Dilution in Aqueous Solution. *Nanoscale* **2018**, *10*, 15904−15910.
(6) Santoyo-Sanchez, M. P.; del Carmen Silva-Lucero, M.; Arreola-Mendoza, L.; Barbier, O. C. Effects of Acute Sodium Fluoride Exposure on Kidney Function, Water Homeostasis, and Renal Handling of Calcium and Inorganic Phosphate. *Biol. Trace Elem. Res.* **2013**, *152*, 367−372.
(7) Otting, G. Prospects for Lanthanides in Structural Biology by NMR. *J. Biomol. NMR* **2008**, *42*, 1−9.
(8) Mindell, J. A. Lysosomal Acidification Mechanisms. *Annu. Rev. Physiol.* **2012**, *74*, 69−86.
(9) Bogdan, N.; Vetrone, F.; Ozin, G. A.; Capobianco, J. A. Synthesis of Ligand-Free Colloidally Stable Water Dispersible Brightly Luminescent Lanthanide-Doped Upconverting Nanoparticles. *Nano Lett.* **2011**, *11*, 835−840.
(10) Barbier, O.; Arreola-Mendoza, L.; Del Razo, L. M. Molecular Mechanisms of Fluoride Toxicity. *Chem.-Biol. Interact.* **2010**, *188*, 319−333.
(11) Shannahan, J. H.; Podila, R.; Aldossari, A. A.; Emerson, H.; Powell, B. A.; Ke, P. C.; Rao, A. M.; Brown, J. M. Formation of a Protein Corona on Silver Nanoparticles Mediates Cellular Toxicity via Scavenger Receptors. *Toxicol. Sci.* **2015**, *143*, 136−146.
(12) Ahsan, S. M.; Rao, C. M.; Ahmad, M. F. Nanoparticle-Protein Interaction: The Significance and Role of Protein Corona BT - *Cellular and Molecular Toxicology of Nanoparticles*; Saquib, Q., Faisal, M., Al-Khedhairy, A. A., Alatar, A. A., Eds.; Springer International Publishing: Cham, 2018; pp 175−198.
(13) Voutchkova, A. M.; Osimitz, T. G.; Anastas, P. T. Toward a Comprehensive Molecular Design Framework for Reduced Hazard. *Chem. Rev.* **2010**, *110*, 5845−5882.
(14) Li, R.; Ji, Z.; Dong, J.; Chang, C. H.; Wang, X.; Sun, B.; Wang, M.; Liao, Y.-P.; Zink, J. I.; Nel, A. E.; et al. Enhancing the Imaging and Biosafety of Upconversion Nanoparticles through Phosphonate Coating. *ACS Nano* **2015**, *9*, 3293−3306.
(15) Recalde, I.; Estebanez, N.; Francés-Soriano, L.; Liras, M.; González-Béjar, M.; Pérez-Prieto, J. Upconversion Nanoparticles with a Strong Acid-Resistant Capping. *Nanoscale* **2016**, *8*, 7588−7594.
(16) Plenio, H. The Coordination Chemistry of the CF Unit in Fluorocarbons. *Chem. Rev.* **1997**, *97*, 3363−3384.
(17) Plenio, H. The Coordination Chemistry of Fluorine in Fluorocarbons. *ChemBioChem* **2004**, *5*, 650−655.

DOI: 10.1021/acsomega.8b03015
ACS Omega 2019, 4, 3012−3019

(18) Perutz, R. N. A Catalytic Foothold for Fluorocarbon Reactions. *Science* **2008**, *321*, 1168.
(19) Burdeniuc, J.; Jedicka, B.; Crabtree, R. H. Recent Advances in C−F Bond Activation. *Eur. J. Inorg. Chem.* **2006**, *130*, 145−154.
(20) San Filippo, J., Jr.; Nuzzo, R. G.; Romano, L. J. Application of Lanthanide Shift Reagents to Alkyl Fluorides. *J. Am. Chem. Soc.* **1975**, *97*, 2546.
(21) Träff, A. M.; Janjetovic, M.; Ta, L.; Hilmersson, G. Selective C-F Bond Activation: Substitution of Unactivated Alkyl Fluorides Using YbI3. *Angew. Chem. Int. Ed.* **2013**, *52*, 12073−12076.
(22) Janjetovic, M.; Träff, A. M.; Hilmersson, G. Mild and Selective Activation and Substitution of Strong Aliphatic C-F Bonds. *Chem. - Eur. J.* **2015**, *21*, 3772−3777.
(23) Wilhelm, S.; Kaiser, M.; Würth, C.; Heiland, J.; Carrillo-Carrion, C.; Muhr, V.; Wolfbeis, O. S.; Parak, W. J.; Resch-Genger, U.; Hirsch, T. Water Dispersible Upconverting Nanoparticles: Effects of Surface Modification on Their Luminescence and Colloidal Stability. *Nanoscale* **2015**, *7*, 1403−1410.
(24) Dong, A.; Ye, X.; Chen, J.; Kang, Y.; Gordon, T.; Kikkawa, J. M.; Murray, C. B. A Generalized Ligand-Exchange Strategy Enabling Sequential Surface Functionalization of Colloidal Nanocrystals. *J. Am. Chem. Soc.* **2011**, *133*, 998−1006.
(25) Muhr, V.; Würth, C.; Kraft, M.; Buchner, M.; Baeumner, A. J.; Resch-Genger, U.; Hirsch, T. Particle-Size-Dependent Förster Resonance Energy Transfer from Upconversion Nanoparticles to Organic Dyes. *Anal. Chem.* **2017**, *89*, 4868−4874.
(26) Pavia, D. L.; Lampman, G. M.; Kriz, G. S. *Introduction to Spectroscopy: A Guide for Students of Organic Chemistry*; Saunders Golden Sunburst Series; Harcourt College Publishers, 2001.
(27) Mishra, S. K.; Suryaprakash, N. Intramolecular Hydrogen Bonding Involving Organic Fluorine: NMR Investigations Corroborated by DFT-Based Theoretical Calculations. *Molecules* **2017**, *22*, 423.
(28) Güizado-Rodríguez, M.; Ariza-Castolo, A.; Merino, G.; Vela, A.; Noth, H.; Bakhmutov, V. I.; Contreras, R. Weak Intramolecular Proton−Hydride and Proton−Fluoride Interactions: Experimental (NMR, X-Ray) and DFT Studies of the Bis(NBH_3) and Bis(NBF_3) Adducts of 1,3-Dimethyl-1,3-Diazolidine. *J. Am. Chem. Soc.* **2001**, *123*, 9144−9152.
(29) Das, G. K.; Stark, D. T.; Kennedy, I. M. Potential Toxicity of Up-Converting Nanoparticles Encapsulated with a Bilayer Formed by Ligand Attraction. *Langmuir* **2014**, *30*, 8167−8176.
(30) Boyer, J.-C.; Manseau, M.-P.; Murray, J. I.; van Veggel, F. C. J. M. Surface Modification of Upconverting NaYF4 Nanoparticles with PEG−Phosphate Ligands for NIR (800 nm) Biolabeling within the Biological Window. *Langmuir* **2010**, *26*, 1157−1164.
(31) Plohl, O.; Kralj, S.; Majaron, B.; Fröhlich, E.; Ponikvar-Svet, M.; Makovec, D.; Lisjak, D. Amphiphilic Coatings for the Protection of Upconverting Nanoparticles against Dissolution in Aqueous Media. *Dalton Trans.* **2017**, *46*, 6975−6984.

DOI: 10.1021/acsomega.8b03015
ACS Omega 2019, 4, 3012−3019